

Figure S1. (A-B) Representative ROS staining images of human and rat femoral head samples. (C) Representative IF co-staining images of CD90 and GPX4 of human femoral head samples. (D) Representative TUNEL staining images of human femoral head samples. (E-F) Quantitative analysis of ROS staining of human and rat femoral head samples (n = 5). (G-H) Quantitative analysis of TUNEL staining of human and rat femoral head samples (n = 5). Data are presented as mean \pm SD. *** $P < 0.001$ (vs. GONFH).

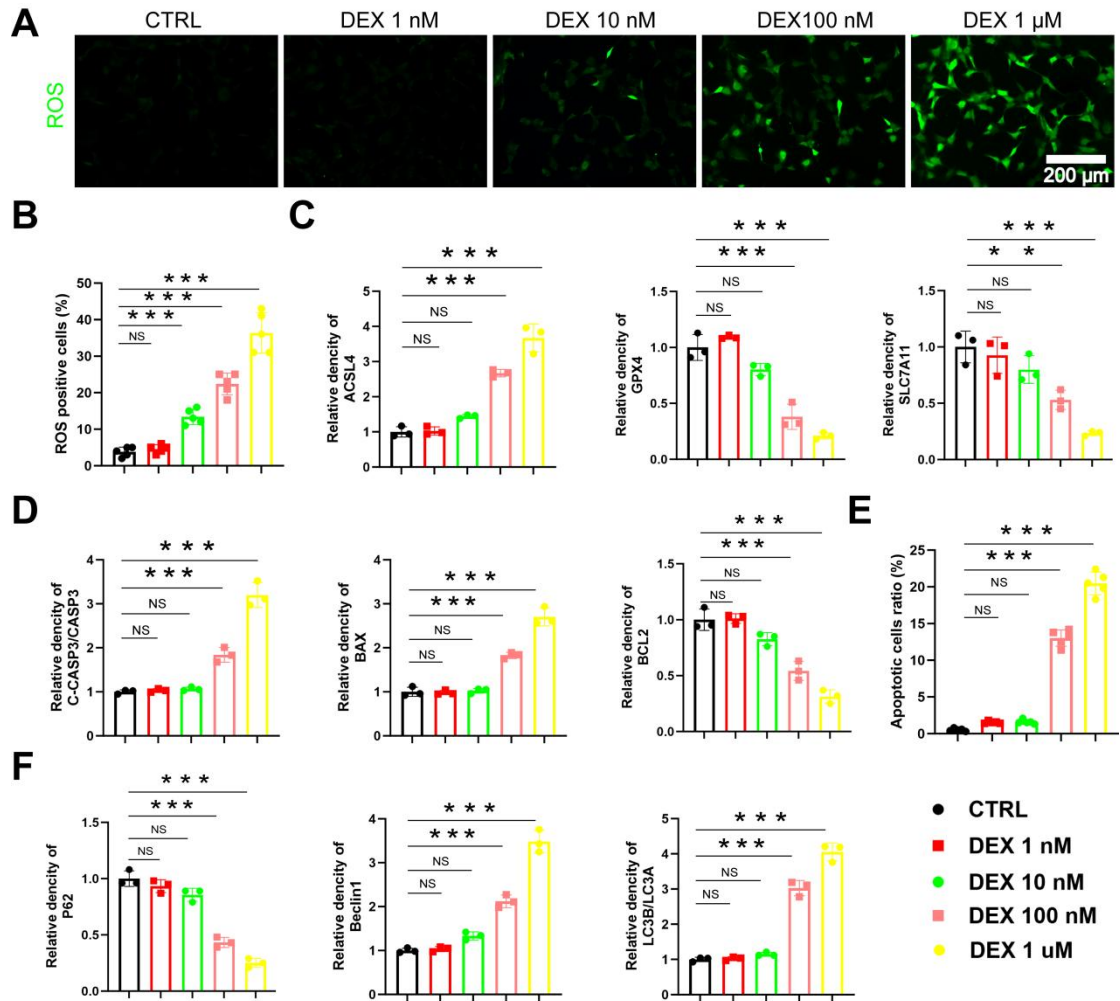


Figure S2. (A-B) Representative ROS staining images and quantitative analysis in BMSCs treated with different concentrations of DEX ($n = 5$). (C) Protein levels of ASCL4, GPX4 and SLC7A11 in BMSCs treated with different concentrations of DEX ($n = 3$). (D) Protein levels of C-CASP3, CASP3, BAX and BCL2 in BMSCs treated with different concentrations of DEX ($n = 3$). (E) Apoptotic ratio of BMSCs treated with different concentrations of DEX ($n = 5$). (F) Protein levels of P62, Beclin1 and LC3B in BMSCs treated with different concentrations of DEX ($n = 3$). Data are presented as mean \pm SD. NS no significance, $**P < 0.01$, and $***P < 0.001$ (vs. CTRL).

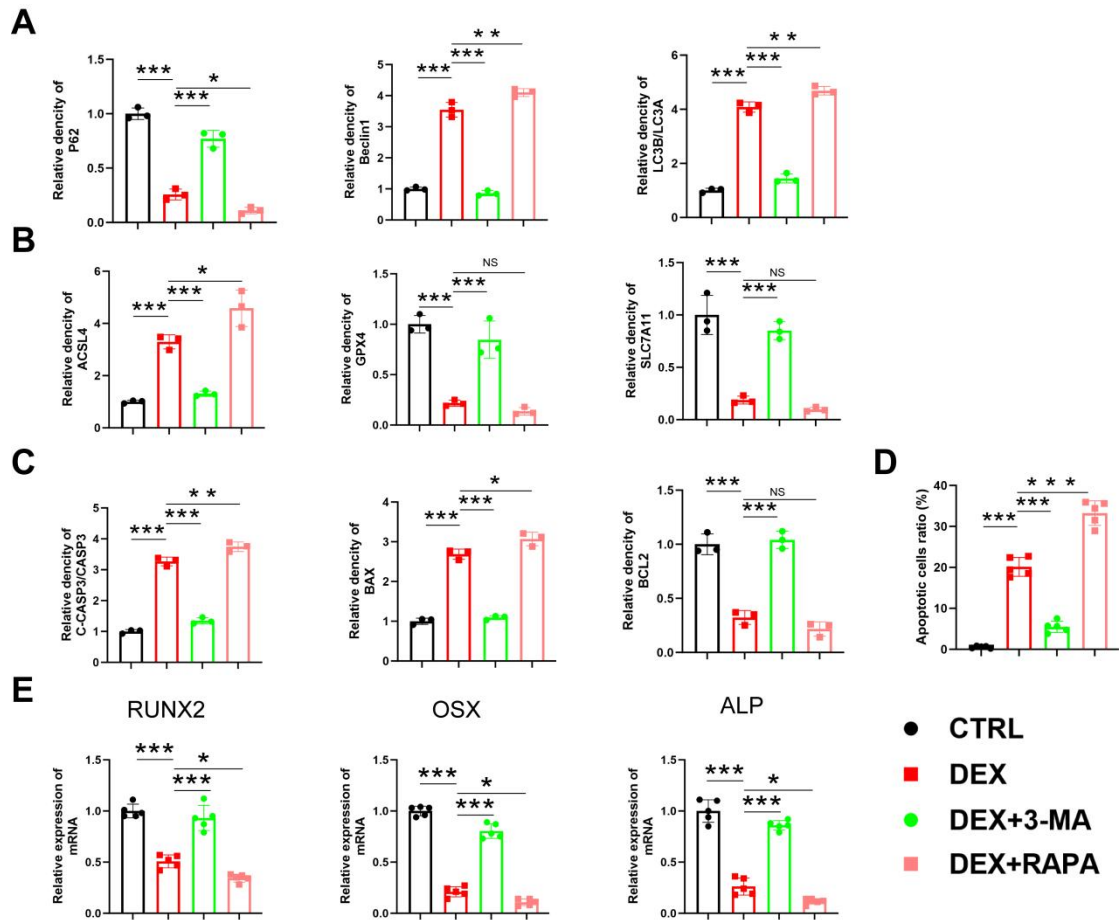


Figure S3. (A-C) Protein levels of P62, Beclin1, LC3B, ACSL4, GPX4, SLC7A11, C-CASP3, CASP3, BAX and BCL2 in 1 μ M DEX or 3-MA or RAPA-treated BMSCs (n = 3). (D) Apoptotic ratio in 1 μ M DEX or 3-MA or RAPA-treated BMSCs (n = 5). (E) mRNA levels of RUNX2, OSX and ALP in 1 μ M DEX or 3-MA or RAPA-treated BMSCs (n = 5). Data are presented as mean \pm SD. NS no significance, * P < 0.05, ** P < 0.01, and *** P < 0.001 (vs. 1 μ M DEX).

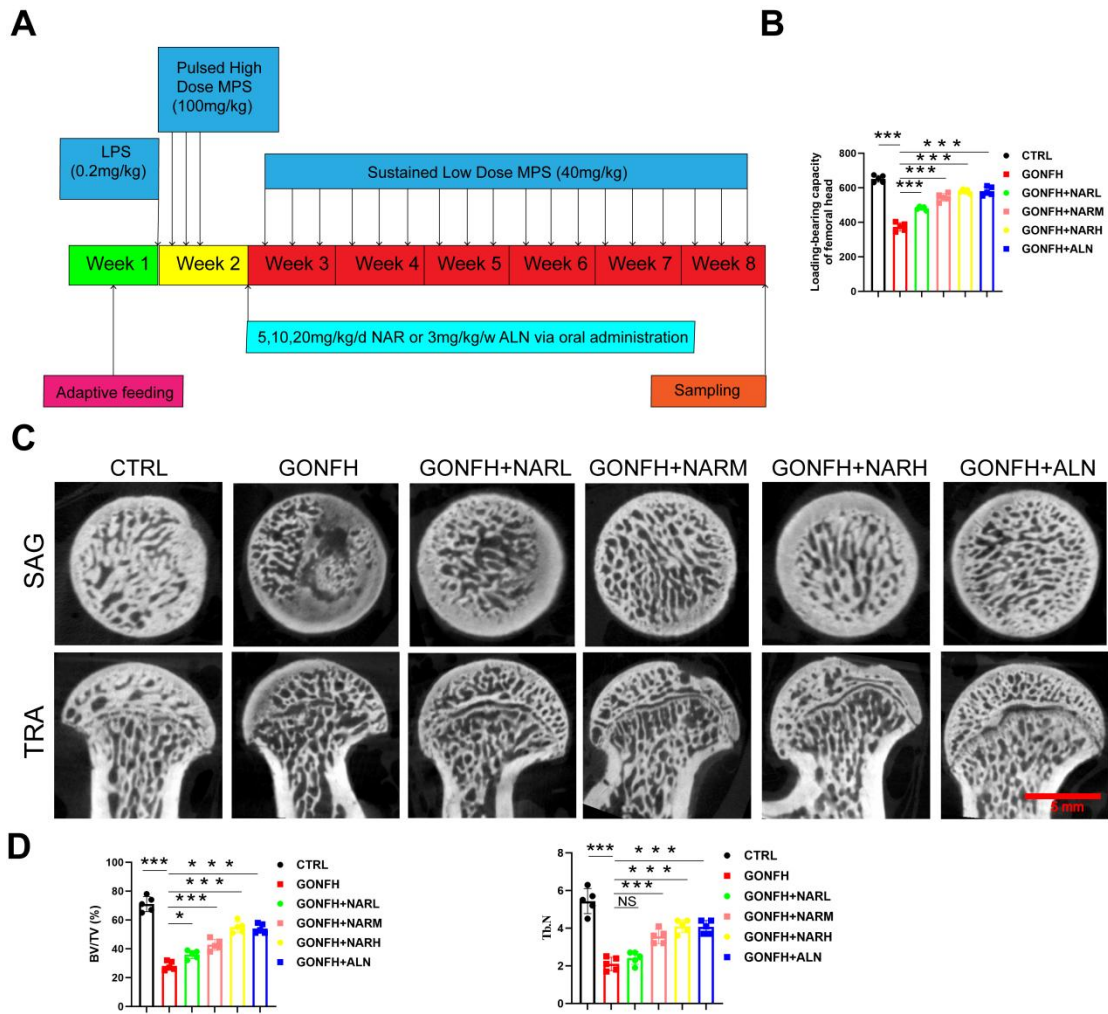


Figure S4. (A) The schematic diagram of the in vivo modelling procedure. (B) The load-bearing capacity of rat femoral head samples ($n = 5$). (C) Representative μ -CT scanning images of rat femoral head samples. (D) Quantitative analysis of BV/TV and Tb.N of rat femoral head samples ($n = 5$). Data are presented as mean \pm SD. NS no significance, $*P < 0.05$, and $***P < 0.001$ (vs. GONFH).

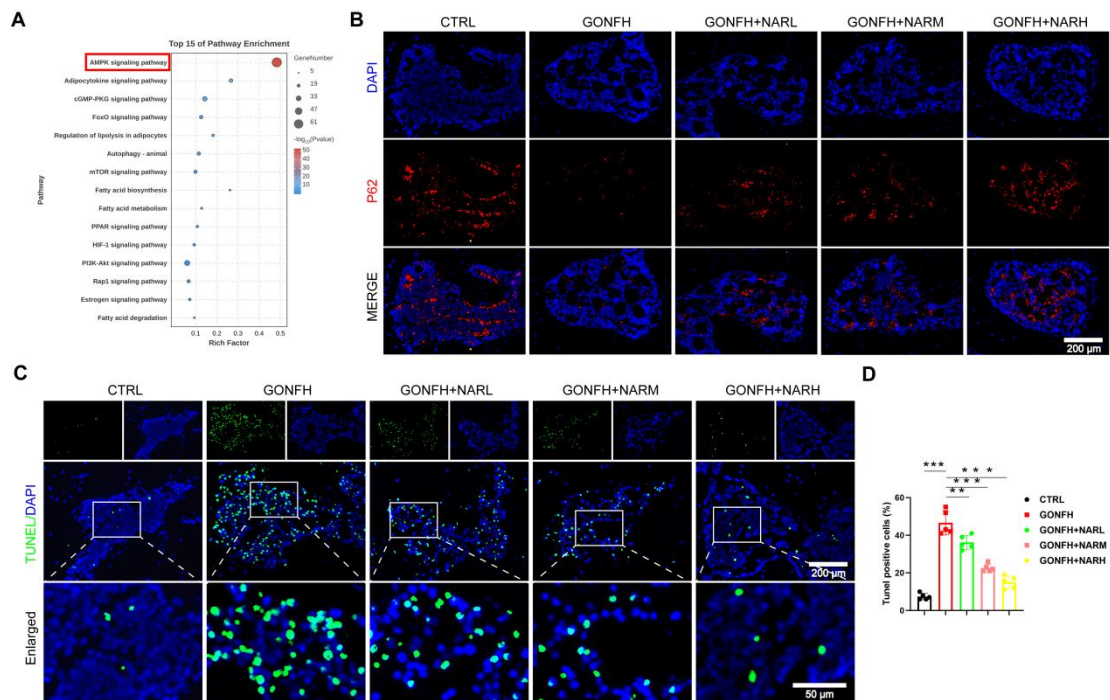


Figure S5. (A) KEGG enrichment analysis plot for RNA sequencing. (B) Representative IF staining images of P62 of rat femoral head samples. (C-D) Representative TUNEL staining images and quantitative analysis of rat femoral head samples ($n = 5$). Data are presented as mean \pm SD. $**P < 0.01$, and $***P < 0.001$ (vs. GONFH).

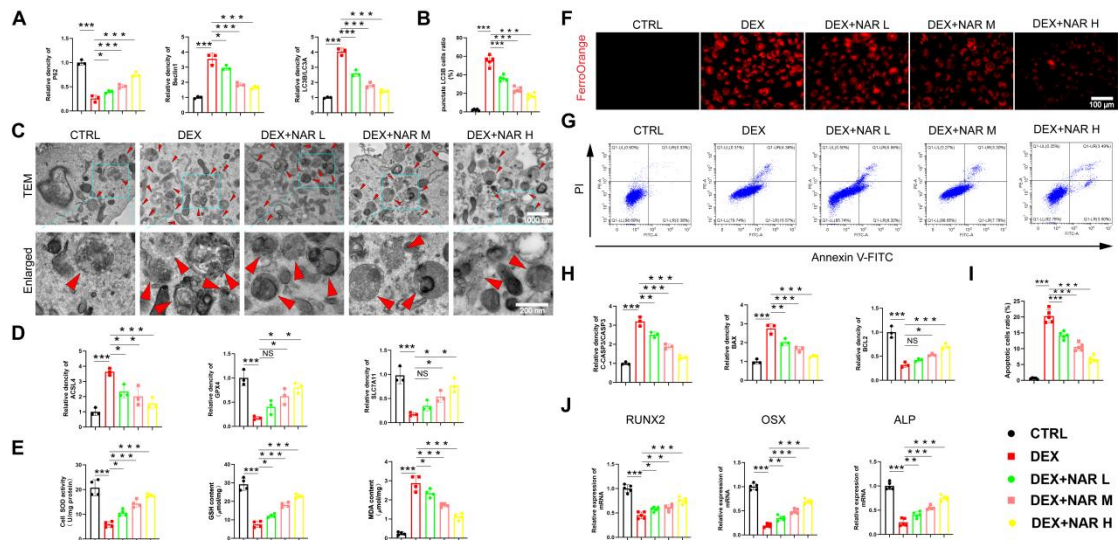


Figure S6. (A) Protein levels of P62, Beclin1 and LC3B in BMSCs treated with 1 μM DEX and different concentrations of NAR (n = 3). (B) Quantitative analysis of mCherry-GFP-LC3B in BMSCs treated with 1 μM DEX and different concentrations of NAR (n = 5). (C) Representative TEM images in BMSCs treated with 1 μM DEX and different concentrations of NAR. (D) Protein levels of ASCL4, GPX4 and SLC7A11 in BMSCs treated with 1 μM DEX and different concentrations of NAR (n = 3). (E) SOD, GSH and MDA levels in BMSCs treated with 1 μM DEX and different concentrations of NAR (n = 4). (F) FerroOrange staining images in BMSCs treated with 1 μM DEX and different concentrations of NAR. (G) Annexin V-FITC/PI assay in BMSCs treated with 1 μM DEX and different concentrations of NAR. (H) Protein levels of C-CASP3, CASP3, BAX and BCL2 in BMSCs treated with 1 μM DEX and different concentrations of NAR (n = 3). (I) Apoptotic ratio in BMSCs treated with 1 μM DEX and different concentrations of NAR (n = 5). (J) mRNA levels of RUNX2, OSX and ALP in BMSCs treated with 1 μM DEX and different concentrations of NAR (n = 5). Data are presented as mean \pm SD. NS no significance, * $P < 0.05$, ** $P < 0.01$, and *** $P < 0.001$ (vs. 1 μM DEX).

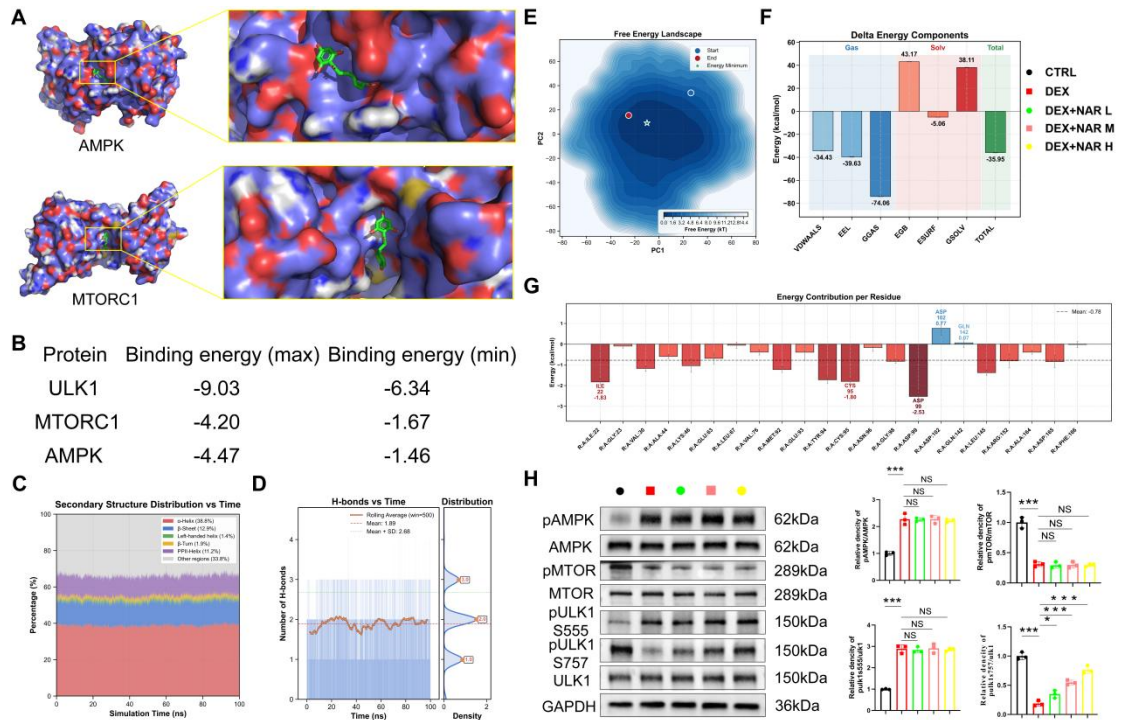


Figure S7. (A) Molecular docking image of NAR with AMPK and MTOR. (B) Molecular docking binding capacity of NAR to ULK1, MTOR and AMPK. (C) ULK1 secondary structure content over time. (D) ULK1-NAR hydrogen bond number plotted over time. (E) Free energy landscape map. (F) Analysis of the binding free energy composition of ULK1-NAR. (G) Residue energy contribution map of ULK1-NAR. (H) The levels of AMPK/MTOR/ULK1 signalling pathway-related proteins in BMSCs treated with 1 μ M DEX and different concentrations of NAR ($n = 3$). Data are presented as mean \pm SD. NS no significance, * $P < 0.05$, and *** $P < 0.001$ (vs. 1 μ M DEX).

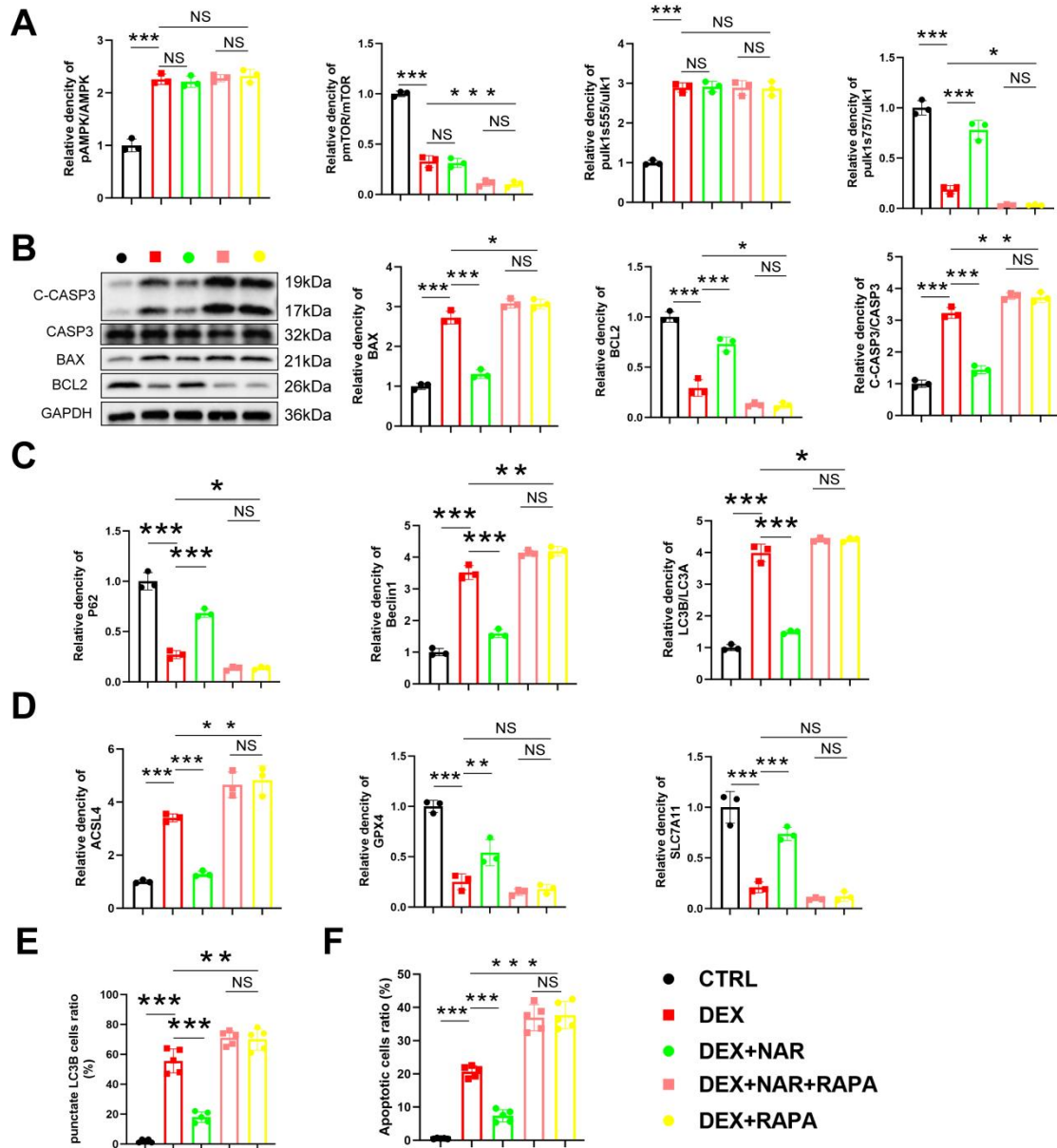


Figure S8. (A) The levels of AMPK/MTOR/ULK1 signalling pathway-related proteins in BMSCs treated with 1 μ M DEX and 20 μ M NAR and RAPA (n = 3). (B) Protein levels of C-CASP3, CASP3, BAX and BCL2 in 1 μ M DEX, 3-MA or RAPA-treated BMSCs (n = 3). (C-D) Protein levels of P62, Beclin1, LC3B, ACSL4, GPX4 and SLC7A11 in BMSCs treated with 1 μ M DEX, 20 μ M NAR and RAPA (n = 3). (E) Quantitative analysis of mCherry-GFP-LC3B in BMSCs treated with 1 μ M DEX, 20 μ M NAR and RAPA (n = 5). (F) Apoptotic ratio in BMSCs treated with 1

μM DEX, 20 μM NAR and RAPA ($n = 5$). Data are presented as mean \pm SD. NS no significance, $*P < 0.05$, $**P < 0.01$, and $***P < 0.001$ (vs. 1 μM DEX or DEX+RAPA).

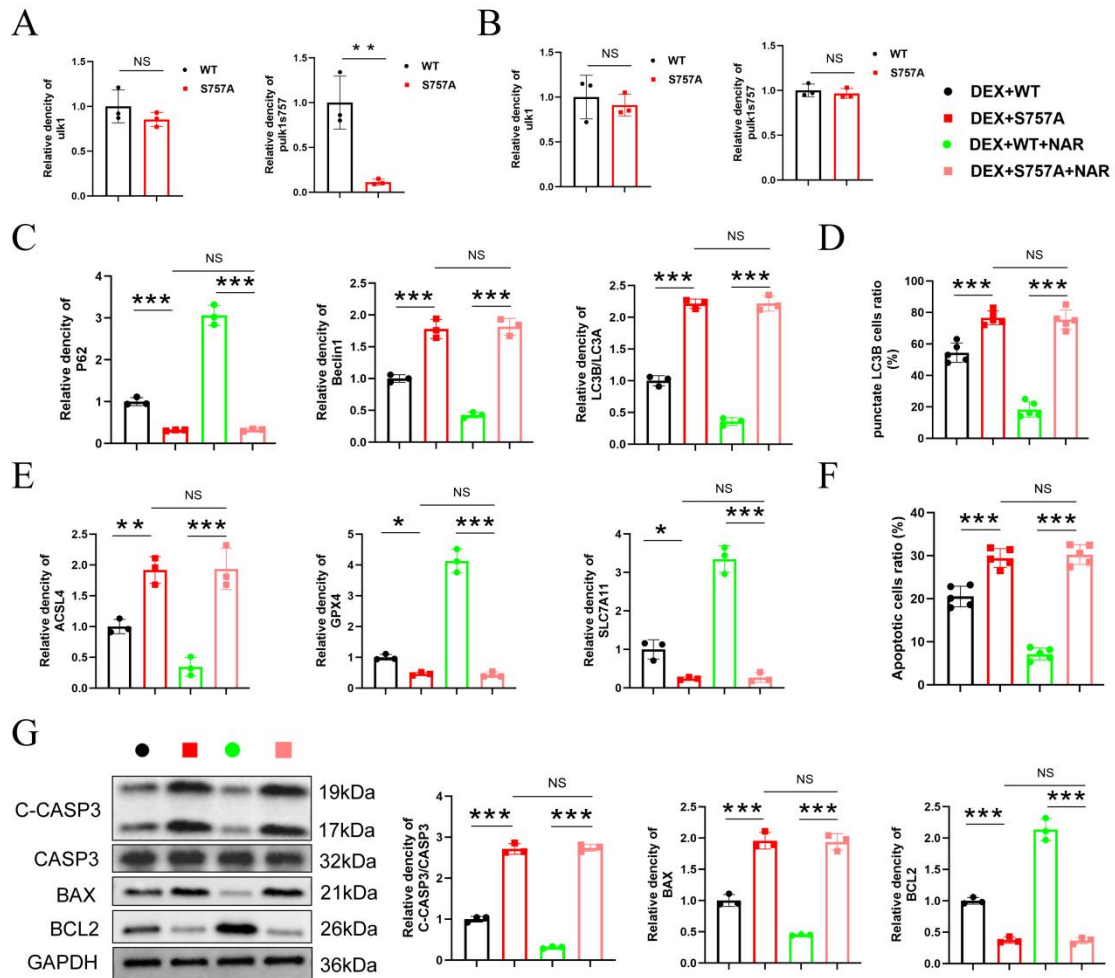


Figure S9. (A-B) Protein levels of ULK1 and pULK1 ser757 in BMSCs treated with S757A and NAR (n = 3). (C) Protein levels of P62, Beclin1 and LC3B in BMSCs treated with 1 μ M DEX and WT or S757A or 20 μ M NAR (n = 3). (D) Quantitative analysis of mCherry-GFP-LC3B in BMSCs treated with 1 μ M DEX and WT or S757A or 20 μ M NAR (n = 5). (E) Protein levels of ACSL4, GPX4 and SLC7A11 in BMSCs treated with 1 μ M DEX and WT or S757A or 20 μ M NAR (n = 3). (F) Apoptotic ratio in BMSCs treated with 1 μ M DEX and WT or S757A or 20 μ M NAR (n = 5). (G) Protein levels of C-CASP3, CASP3, BAX and BCL2 in BMSCs treated with 1 μ M DEX and WT or S757A or 20 μ M NAR (n = 3). Data are presented as mean \pm SD. NS no significance, * P < 0.05, and *** P < 0.001 (vs. DEX+S757A or

DEX+S757A+NAR).

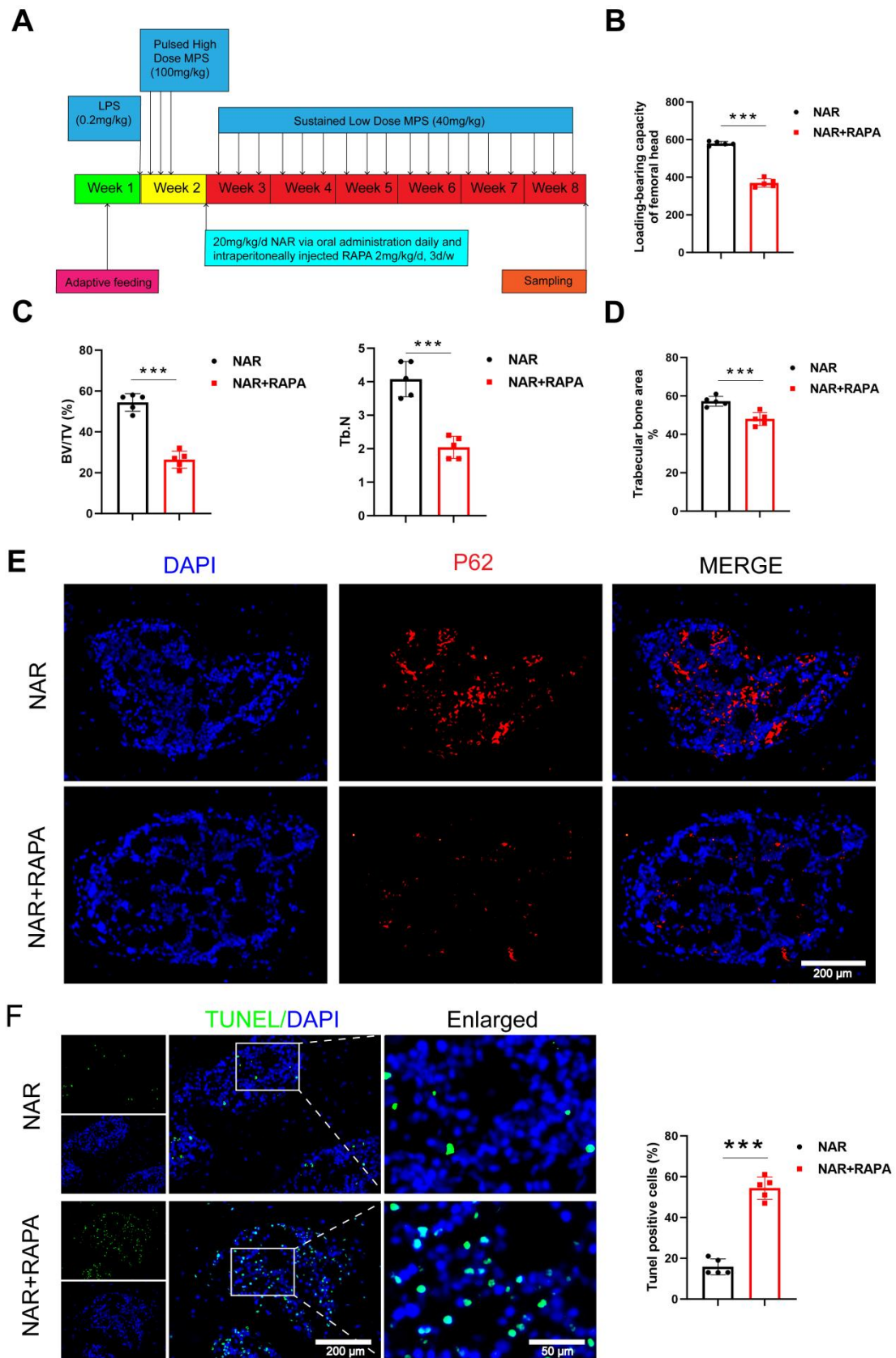


Figure S10. (A) The schematic diagram of the in vivo modelling procedure. (B) The

load-bearing capacity of rat femoral head samples ($n = 5$). (C) Quantitative analysis of BV/TV and Tb.N of rat femoral head samples ($n = 5$). (D) Quantitative analysis of trabecular bone area of rat femoral head samples ($n = 5$). (E) Representative IF staining images of P62 in rat femoral head samples. (F) Representative TUNEL staining images and quantitative analysis of rat femoral head samples ($n = 5$). Data are presented as mean \pm SD. *** $P < 0.001$ (vs. NAR).

Table S1. Antibodies information

Antibodies	Company	Catalog #	Application/Dilution
CD90	Proteintech	66766-1-Ig	IF (1:100)
LC3B	Novus	NB100-2220	IF (1:100); WB (1:1000)
P62	Huabio	R1309-8	IF (1:100); WB (1:1000)
Beclin1	Abclonal	A7353	WB (1:1000)
C-CASP3	Cell Signaling Technology	9664S	WB (1:1000)
CASP3	Huabio	ET1608-64	WB (1:1000)
BAX	Huabio	ET1603-34	WB (1:1000)
BCL2	Huabio	ET1702-53	WB (1:1000)
GPX4	Abclone	A25009	IF (1:200); WB (1:1000)
ACSL4	Abclone	A22901	WB (1:10000)
SLC7A11	Novus	NB300-318	WB (1:1000)
ALP	Arigo	ARG57422	IF (1:100)
pULK1S757	Affinity	AF4387	IF (1:100)
pAMPK	Cell Signaling Technology	2535S	WB (1:1000)
AMPK	Cell Signaling Technology	5832S	WB (1:1000)
pMTOR	Cell Signaling Technology	5536T	WB (1:1000)
MTOR	Cell Signaling Technology	2983S	WB (1:1000)
pULK1S757	Cell Signaling Technology	6888S	WB (1:1000)
pULK1S555	Novus	NBP3-13124	WB (1:1000)
ULK1	Cell Signaling Technology	8054S	WB (1:1000)
GAPDH	Huabio	ET1601-4	WB (1:5000)
Goat anti-Mouse IgG (HRP-conjugated)	Proteintech	SA00001-1	WB (1:5000)
Goat anti-Rabbit IgG (HRP-conjugated)	Proteintech	SA00001-2	WB (1:5000)
Anti-Rabbit IgG for IHC	ZSGB-BIO	PV-6001	IHC (1:1000)
Anti-Mouse IgG for IF	Thermo Fisher Scientific	A11001	IF (1:1000)

Anti-Rabbit IgG
for IF

Thermo Fisher
Scientific

A31572

IF (1:1000)

Table S2. Sequences of primers

Primer name	Sequence
RUNX2 forward	5'-GAGGGCACAAGTTCTATCTGGA-3'
RUNX2 reverse	5'-GGTGGTCCGCGATGATCTC-3'
OSX forward	5'-CCCTTCTCAAGCACCAATGG-3'
OSX reverse	5'-AAGGGTGGGTAGTCATTTGCATA-3'
ALP forward	5'-GTTGGGGGTGCCACGGT-3'
ALP reverse	5'-CCTTGGACAGAGCCATGTATG-3'
β -Actin forward	5'-GGAGATTACTGCCCTGGCTCCTA-3'
β -Actin reverse	5'-GACTCATCGTACTCCTGCTTGCTG-3'